European Journal of Radiology 118 (2019) 44–50

Contents lists available at ScienceDirect

European Journal of Radiology

journal homepage: www.elsevier.com/locate/ejrad

Research article

Value of normalized apparent diffusion coefficients in differentiating between borderline and malignant epithelial ovarian tumors

Jing Lu[a], Shan Pi[a], Feng Hua Ma[b], Shu Hui Zhao[c], Hai Ming Li[a], Shu Lei Cai[b], Jin Wei Qiang[a,*]

[a] Department of Radiology, Jinshan Hospital, Fudan University, 1508 Longhang Road, Shanghai, 201508, PR China
[b] Department of Radiology, Obstetrics and Gynecology Hospital, Fudan University, 419 Fangxie Road, Huangpu District, Shanghai, 200011, PR China
[c] Department of Radiology, Xinhua Hospital, Medical College of Shanghai Jiao Tong University, Shanghai, 200092, PR China

ARTICLE INFO

Keywords:
Ovarian tumor
Borderline
Malignant
Apparent diffusion coefficient
Magnetic resonance imaging

ABSTRACT

Purpose: To compare the diagnostic performance of normalized apparent diffusion coefficients (nADCs) of different references with that of ADCs at different*b* factors in differentiating borderline epithelial ovarian tumors (BEOTs) from malignant epithelial ovarian tumors (MEOTs).

Method: This retrospective study included 53 BEOTs and 148 MEOTs. Conventional magnetic resonance and diffusion-weighted imaging with*b* factors of 800 and 1000s/mm^2 were performed. ADC was measured three times at solid components of tumors, gluteus maximus muscle (GMM), iliopsoas muscle (IM) and urine and then averaged. ADC_{tumor}, nADCs were then obtained. Differences and the diagnostic performance of ADC_{tumor} and nADCs between BEOTs and MEOTs with different *b* factors were compared.

Results: ADC_{tumor}, nADCs regardless of *b* factors were significantly higher in BEOTs than MEOTs. The diagnostic performance of $nADC_{urine}$ regardless of *b* factors was significantly larger than that of $nADC_{GMM}$ and $nADC_{IM}$. There was no significant difference in the diagnostic performance between ADC_{tumor} and $nADC_{urine}$ regardless of *b* factors. A significantly lower ADC_{tumor} and a larger diagnostic performance for ADC_{tumor} was found with a *b* factor of 1000s/mm^2 than 800 s/mm^2. There were no significant differences in $nADC_{urine}$ of BEOTs or MEOTs or in the diagnostic performance of $nADC_{urine}$ with *b* factors between 800 and 1000s/mm^2.

Conclusions: ADC_{tumor} and nADCs were both capable of differentiating BEOTs from MEOTs. $nADC_{urine}$ was the best of all nADCs and was superior to ADC_{tumor} because of its stable performance in differentiating BEOTs from MEOTs, regardless of *b* factors.

1. Introduction

Borderline epithelial ovarian tumors (BEOTs) are neoplasms of low malignant potential [1] that occur in women of all ages, but these women have a mean age of approximately 40 years, which is 15 years younger than women with malignant epithelial ovarian tumors (MEOTs) [2]. A large proportion of patients with BEOTs are of reproductive age, and fertility-sparing surgery, such as either ovarian cystectomy or unilateral salpingo-oophorectomy, can be an optimal choice [2]. Unlike BEOT patients, MEOT patients are more likely to require a comprehensive staging laparotomy and postoperative chemotherapy [3]. Therefore, the accurate preoperative differentiation of BEOTs from MEOTs is crucial for selecting the optimal surgical procedure. However, it is difficult to differentiate BEOTs from MEOTs because of the relative rarity and the absence of a reliable test or marker of BEOTs [2].

BEOT patients are frequently asymptomatic, and these tumors are usually found by ultrasound. However, there are no pathognomonic sonographic appearances associated with BEOTs, which leads to a sensitivity of merely 49% to 63%, a specificity of 57% for this method [2,4,5]. The availability of reliable frozen-section diagnosis is a problem in many hospitals [2], and this technique has an accuracy of 60% to 75% [6]. Computed tomography (CT) is not capable of differentiating BEOTs from MEOTs because CT has poor soft tissue contrast [7]. Magnetic resonance imaging (MRI) plays a vital role in the characterization of ovarian tumors. However, previous studies indicated that BEOTs share many morphological features with MEOTs on conventional MRI, which makes determining a differential diagnosis difficult [7–11]. Diffusion-weighted imaging (DWI) is able to detect cellularity and cell membrane integrity by using the apparent diffusion coefficient (ADC) to quantify the diffusion of water molecules in tissues [12]. Highly cellular tumors are more likely to have restricted diffusion

* Corresponding author.
E-mail address: dr.jinweiqiang@163.com (J.W. Qiang).

https://doi.org/10.1016/j.ejrad.2019.06.020
Received 8 May 2019; Received in revised form 21 June 2019; Accepted 25 June 2019

than slightly cellular tumors [13]. Previous studies have demonstrated the important role of ADCs in differentiating BEOTs from MEOTs [13–17]. BEOTs display a lower DWI signal intensity (SI) and higher ADC values than MEOTs. Nevertheless, the differential cut-off ADC values vary across different studies owing to many factors, such as the *b* factor, location and area of the region of interest (ROI), patient age, and body temperature [18]. According to a meta-analysis of the diagnostic performance of ADC values in differentiating between BEOTs and MEOTs, the *b* factor was the main source of heterogeneity [12]. The normalized apparent diffusion coefficient (nADC) calculated by the formula $ADC_{tumor}/ADC_{reference}$ has been applied to reduce the variance of ADCs in glioma, liver fibrosis, pancreatic lesions and cervical cancer [18–21]. To the best of our knowledge, the value of nADCs in differentiating between BEOTs and MEOTs has not been investigated. Therefore, the purpose of this study was to compare the diagnostic performance of nADCs with different references to that of ADCs with different *b* factors to differentiate BEOTs from MEOTs and to determine the ideal reference ADC for nADCs.

2. Material and methods

2.1. Study population

This retrospective study was approved by our institutional review boards, and informed consent was waived for all patients. From December 2010 to February 2019, one hundred fifty-seven patients with histologically proven BEOTs or MEOTs were included, including 44 BEOT patients with 53 tumors and 113 MEOT patients with 148 tumors.

2.2. MRI technique

MRI was performed using a 1.5 T scanner (Avanto, Siemens, Erlangen, Germany) with a phased array coil. The patients were placed in the supine position and could breathe freely during the acquisition. The scanning protocol is listed in Table 1. Based on the different diffusion gradient *b* factors, the patients were divided into three groups: $Group_{b=800}$, $Group_{b=}$800,1000 and $Group_{b=1000}$. Conventional nonenhanced, DWI and contrast-enhanced scans were performed sequentially. ADC maps were automatically generated with $b = 800\ s/mm^2$ in $Group_{b=800}$ and $b = 1000s/mm^2$ in $Group_{b=1000}$ and $Group_{b=}$800,1000. As ADC maps were automatically generated only at the highest *b* value in $Group_{b=}$800,1000, ADC maps at $b = 800\ s/mm^2$ were manually generated using Dynamic Analysis software provided by the manufacturer (Syngo, Siemens, Erlangen, Germany). After completing the DWI acquisition, a gadolinium chelate (Gd-DTPA, Magnevist; Bayer Schering, Berlin, Germany) was administered at a dose of 0.2 mL/kg. The imaging range was from the inferior pubic symphysis to the renal hilum and was extended beyond the dome of the tumor in cases of large masses.

Table 1
MRI parameters.

Parameters	T1WI	T2WI	T1WI-FS	DWI
Sequence	Turbo SE	Turbo SE	Spoiled GRE	EPI
Repetition time (msec)	340	8000	196	3200
Echo time (msec)	10	83	2.9	87
Section thickness (mm)	5	5	5	5
Intersection gap (mm)	1.5	1.5	1.5	1.5
Field of view (mm)	238 × 280	238 × 280	238 × 280	238 × 280
Matrix	480 × 640	256 × 256	256 × 256	128 × 128
Acquisition time (sec)	120	175	40	166
Diffusion gradient *b* factors (s/mm^2)	–	–	–	0, 800 0, 800, 1000 0, 1000

T1WI: T1-weighted imaging; T2WI: T2-weighted imaging; FS: fat saturation; DWI: diffusion-weighted imaging; SE: spin echo; GRE: gradient echo; EPI: echo planar imaging.

2.3. Quantitative image analysis

The MR images were independently analyzed by two radiologists (radiologists 1 and 2, both with more than five years of experience in gynecological imaging) who were blinded to the patients' clinical data and histopathology results. The SI of the tumor on the DWI scans was classified as high (similar to the SI of the nerve root), moderate (similar to the SI of the small intestine) or low (lower than the SI of the small intestine). The ADC value was measured on the largest tumor slice of the DWI scan, and an elliptical ROI that was drawn to be as large as possible (2.04-6398 mm^2, mean 340.45 mm^2) was placed at the solid component of the tumor, which included the solid portion, papillary projection and thickened wall or septum (> 5 mm), by referring to the conventional MRI scan and carefully avoiding areas of hemorrhage and necrosis, and major vascular structures (Figs. 1 and 2). Then, the ROI was copied to the ADC map to obtain a mean ADC value. The process was repeated three times, and three mean ADC values were averaged as the ADC_{tumor}. The criteria for an appropriate reference for the nADC included the following two conditions: 1) the anatomic border of the reference should be clear, and 2) the reference should provide high interobserver reproducibility for ADC measurements. Therefore, our primary candidates for the reference area included the gluteus maximus muscle (GMM), iliopsoas muscle (IM) and urine. On the contrast-enhanced T1-weighted images, an elliptical ROI drawn as large as possible was placed at the homogeneous SI areas of the GMM (116.69-577.405 mm^2, mean 278.51 mm^2) and IM (59.88-280.90 mm^2, mean 154.58 mm^2) while avoiding fat, calcifications, and vascular structures. Then, the ROI was copied to the ADC map. The measurement was performed three times and averaged. An elliptical ROI drawn as large as possible (6.95-1556.3 mm^2, mean 170.73 mm^2) was placed at the center of the bladder lumen on the ADC maps to measure the mean ADC value, this process was repeated three times, and the three values were averaged. To assess intraobserver variability, the ADC values were measured repeatedly by radiologist 1 after an interval of one month. The nADC was calculated as $ADC_{tumor}/ADC_{reference}$, and the $nADC_{GMM}$, $nADC_{IM}$ and $nADC_{urine}$ were obtained based on the first measurements by radiologist 1. All ADC measurements were performed using a dicom viewer software (RadiAnt DICOM VIEWER (64-bit), Medixant Company, Poznan, Poland).

2.4. Statistical analysis

Statistical analyses were performed with SPSS software (version 23.0, SPSS, Inc., Chicago, IL, USA) for Windows. Continuous variables were presented as arithmetic means and standard deviations (SDs). The intra- and interclass correlation coefficients (ICC) were calculated to evaluate intra- and interobserver variabilities (ICC: 0.00-0.20, poor correlation; 0.21-0.40, fair; 0.41-0.60, moderate; 0.61-0.80, good; and 0.81-1.00, excellent). Two independent-sample *t*-tests or Mann-Whitney U tests were performed to compare the differences between BEOTs and MEOTs in ADC_{tumor} and nADC values depending on if the data were consistent with a normal distribution and if there was homogeneity of variance. Receiver operating characteristic (ROC) curve analysis (MedCalc Software, Mariakerke, Belgium) was used to assess the diagnostic performance and determine a cut-off value for the ADC_{tumor} and nADC to discriminate between BEOTs and MEOTs. A paired-samples *t* test or Wilcoxon signed-ranks test was performed for $Group_{b=}$800,1000 to compare the differences in ADC_{tumor} and nADCs with *b* factors between 800 s/mm^2 and 1000s/mm^2, depending on if the data were consistent with a normal distribution. The Z test was used to compare differences in the area under the curve (AUC) of each ADC value for determining a differential diagnosis. A *P* value less than 0.05 was regarded as statistically significant.

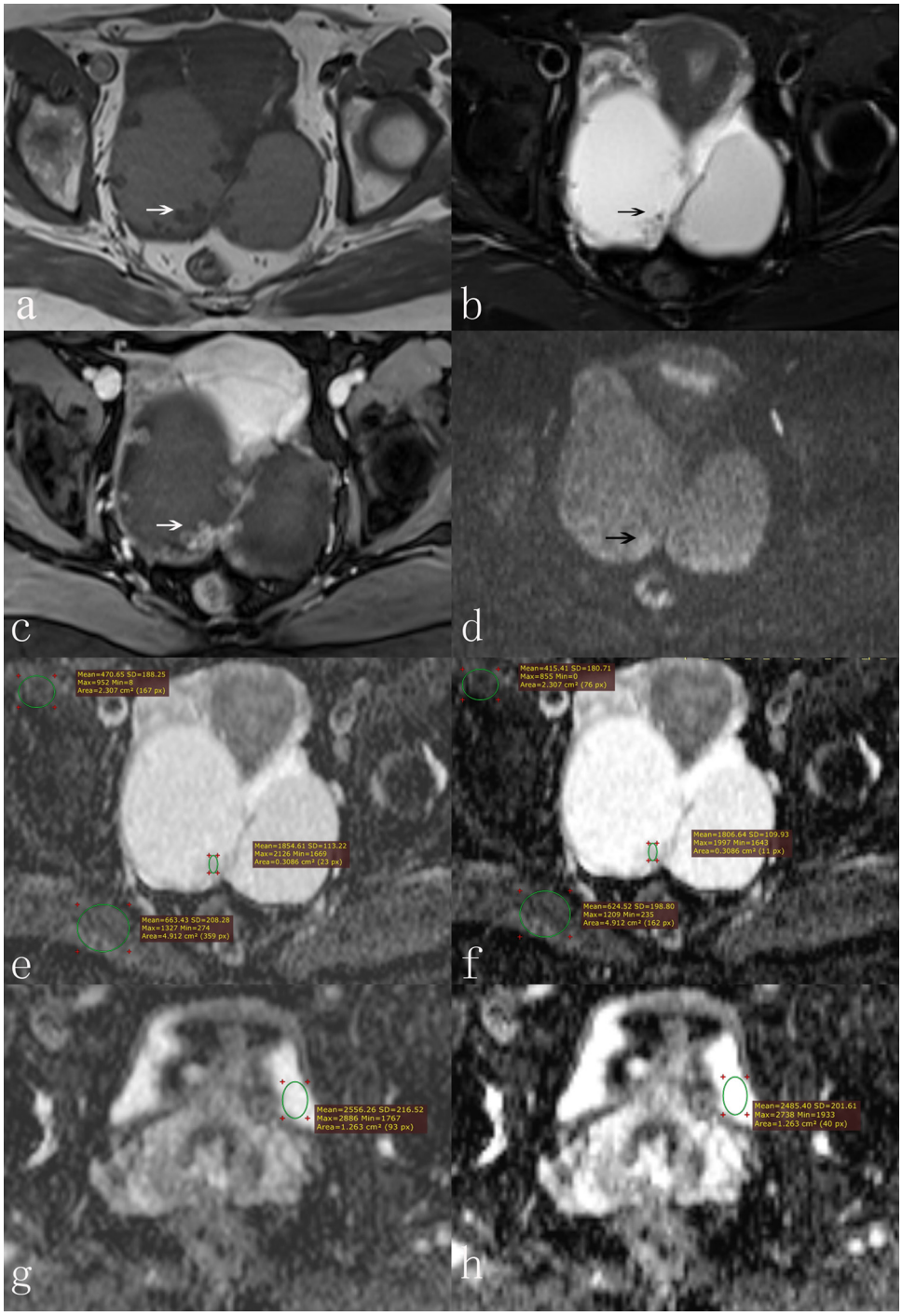

Fig. 1. A 55-year-old woman with bilateral serous borderline ovarian tumors. Axial T1-weighted (a), T2-weighted (b) and T1-weighted contrast-enhanced images (c) show a bilateral unilocular cystic mass with papillary projections that demonstrate enhancement (arrow). An ROI drawn as large as possible was placed on the solid components of tumor and gluteus maximus muscles (GMMs) and iliopsoas muscles (IMs) with homogeneous signal intensity (SI) and on the urine. The papillary projections show moderate SI on the DWI scans (d) and have an ADC_{tumor} value of 1.855×10^{-3} mm^2/s at $b = 800\ s/mm^2$ (e) and 1.807×10^{-3} mm^2/s at $b = 1000s/mm^2$ (f). The ADC_{GMM}, ADC_{IM} and ADC_{urine} are 0.663×10^{-3} mm^2/s, 0.471×10^{-3} mm^2/s and 2.556×10^{-3} mm^2/s at $b = 800\ s/mm^2$, respectively (e, g). Thus, the $nADC_{GMM}$, $nADC_{IM}$ and $nADC_{urine}$ values are 2.798, 3.938 and 0.726, respectively. At $b = 1000s/mm^2$, the ADC_{GMM}, ADC_{IM} and ADC_{urine} are 0.625×10^{-3} mm^2/s, 0.415×10^{-3} mm^2/s and 2.485×10^{-3} mm^2/s, respectively (f, h). The $nADC_{GMM}$, $nADC_{IM}$ and $nADC_{urine}$ are 2.891, 4.354 and 0.727, respectively.

3. Results

Forty-four BEOT patients with 53 tumors and 113 MEOT patients with 148 tumors were included. The patients with BEOTs were aged between 18–70 years (mean, 35.95 years) and those with MEOTs were aged 26–80 years (mean, 51.70 years), and there was a significant difference ($P < 0.001$). The histology types are listed in Table 2. There were 132 cases of ADC maps with $b = 800\ s/mm^2$ and 132 cases with $b = 1000s/mm^2$.

3.1. ADC_{tumor} and nADC values of BEOTs and MEOTs

The intra- and interobserver agreements were excellent in measuring the ADC values of ovarian tumors, with ICCs of 0.947 (95% confidence interval (CI), 0.926, 0.962) and 0.950 (95% CI, 0.923, 0.971), respectively. The intra- and interclass ICCs for $nADC_{GMM}$, $nADC_{IM}$ and $nADC_{urine}$ in all ovarian tumors were 0.735 (95% CI, 0.615, 0.821), 0.892 (95% CI, 0.838, 0.928) and 0.920 (95% CI, 0.872, 0.951) as well as 0.779 (95% CI, 0.607, 0.882), 0.862 (95% CI, 0.678, 0.936) and 0.954 (95% CI, 0.900, 0.979), respectively.

Comparisons of the ADC_{tumor} and nADC values of BEOTs and MEOTs are listed in Table 3. The ADC_{tumor}, $nADC_{GMM}$, $nADC_{IM}$ and $nADC_{urine}$ of BEOTs were significantly higher than those of MEOTs with $b = 800\ s/mm^2$ and $1000s/mm^2$ ($P < 0.001$, $P = 0.001$, $P = 0.008$, $P < 0.001$; and $P < 0.001$, $P < 0.001$, $P = 0.003$, $P < 0.001$, respectively).

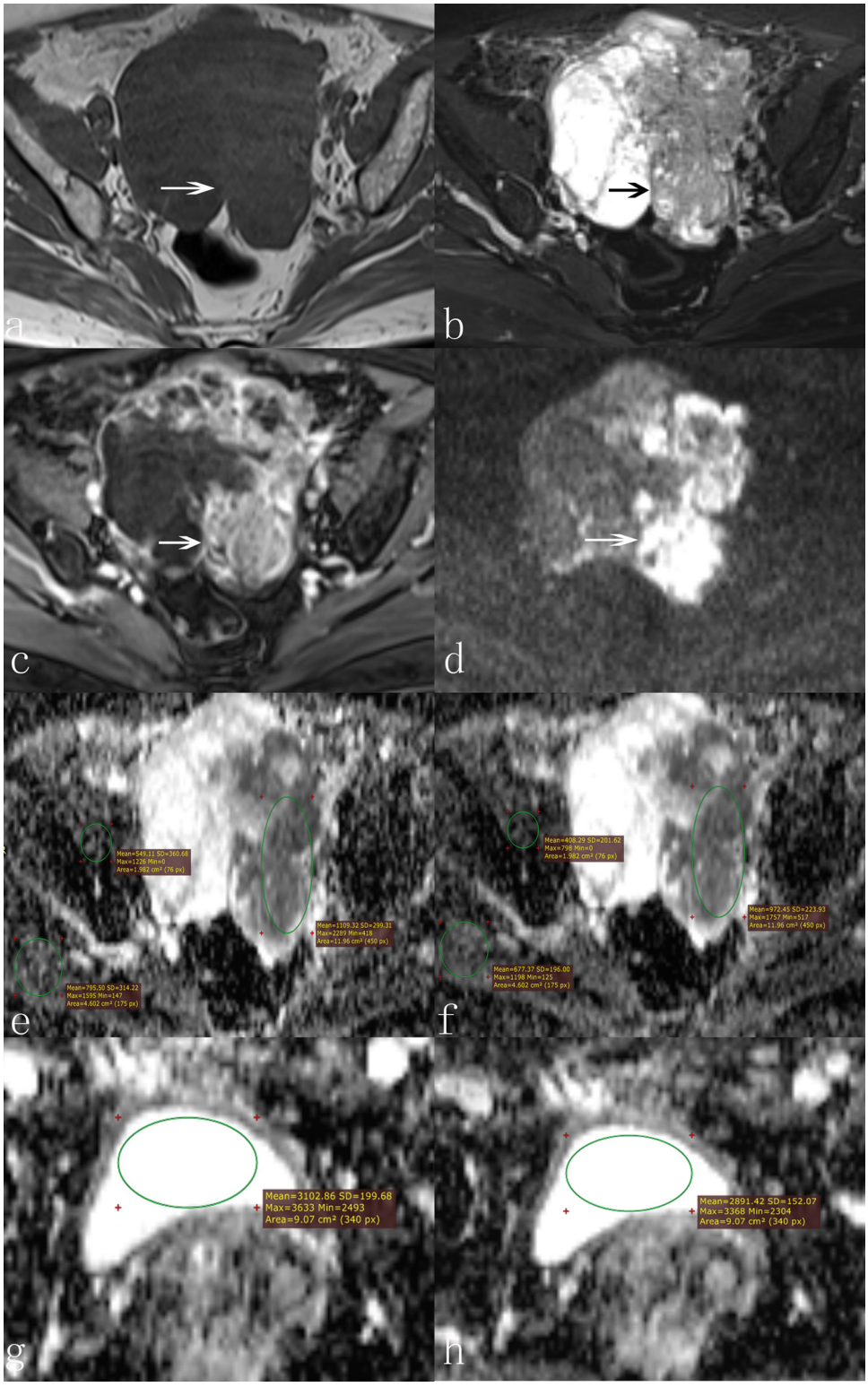

Fig. 2. A 75-year-old woman with poorly differentiated serous ovarian adenocarcinoma. Axial T1-weighted (a), T2-weighted (b) and T1-weighted contrast-enhanced images (c) show a mixed cystic-solid mass (arrow). An ROI drawn as large as possible was placed on the solid components of the tumor and gluteus maximus muscles (GMMs) and iliopsoas muscles (IMs) with homogeneous signal intensity and on the urine. The solid components show high SI on the DWI scan (d) and have an ADC_{tumor} value of 1.109×10^{-3} mm^2/s at $b = 800\ s/mm^2$ (e) and 0.972×10^{-3} mm^2/s at $b = 1000s/mm^2$ (f). The ADC_{GMM}, ADC_{IM} and ADC_{urine} are 0.796×10^{-3} mm^2/s, 0.549×10^{-3} mm^2/s and 3.103×10^{-3} mm^2/s at $b = 800\ s/mm^2$, respectively (e, g). Thus, the $nADC_{GMM}$, $nADC_{IM}$ and $nADC_{urine}$ are 1.393, 2.020 and 0.357, respectively. At $b = 1000s/mm^2$, the ADC_{GMM}, ADC_{IM} and ADC_{urine} are 0.677×10^{-3} mm^2/s, 0.408×10^{-3} mm^2/s and 2.891×10^{-3} mm^2/s, respectively (f, h), and the $nADC_{GMM}$, $nADC_{IM}$ and $nADC_{urine}$ are 1.436, 2.382 and 0.336, respectively.

3.2. Diagnostic performances of ADC_{tumor} and nADCs in differentiating between BEOTs and MEOTs

In terms of differentiating BEOTs from MEOTs, the ROC analysis (Fig. 3) showed that the AUC of $nADC_{urine}$ was significantly larger than that of $nADC_{GMM}$ and $nADC_{IM}$ with a b factor of 800 s/mm^2 and 1000s/mm^2 (all $P < 0.001$, Table 4). The optimal cut-off $nADC_{urine}$ value was 0.415, with a sensitivity of 100%, a specificity of 91.26% and an AUC of 0.987 when $b = 800\ s/mm^2$; the cut-off was 0.406, with a sensitivity of 100%, a specificity of 96.87% and an AUC of 0.992 when $b = 1000s/mm^2$. There were no significant differences in the AUCs between ADC_{tumor} and $nADC_{urine}$ at $b = 800$ and $1000s/mm^2$ ($P = 0.055$ and 0.09, respectively). There were no significant differences in the AUCs of ADC_{tumor} ($P = 0.61$) and $nADC_{urine}$ ($P = 0.83$) between $b = 800\ s/mm^2$ and $1000s/mm^2$. There was a significant difference in age between $Group_{b=800}$ and $Group_{b=1000}$ (49.95 ± 11.75 years vs. 46.43 ± 12.53 years, $P = 0.02$).

Table 2
Histology types of epithelial ovarian tumors in groups with different *b* factors.

Histology types	$Group_{b=800}$	$Group_{b=800,1000}$	$Group_{b=1000}$
BEOT	17	12	24
Serous	12	11	18
Mucinous	5	1	5
Endometrioid	0	0	1
MEOT	52	51	45
Serous	34	43	35
Mucinous	2	3	1
Endometrioid	5	2	3
Clear cell	11	2	5
Mixed	0	1	1
Total	69	63	69

BEOT: borderline epithelial ovarian tumor; MEOT: malignant epithelial ovarian tumor.

3.3. ADC_{tumor} and $nADC_{urine}$ values and their diagnostic performances with a b factor of 800 s/mm² and 1000s/mm² in $Group_{b=800,1000}$

In Group $_{b=}$800,1000, the ADC_{tumor} of BEOTs and MEOTs when b = 1000s/mm² were significantly lower than those when b = 800 s/mm² (P = 0.02 and P < 0.001, respectively, Table 5). In terms of differentiating BEOTs from MEOTs, the AUC of ADC_{tumor} was significantly larger when b = 1000s/mm² than when b = 800 s/mm² (P = 0.03). In $Group_{b=}$800,1000, there were no significant differences between b = 800 s/mm² and b = 1000s/mm² in the $nADC_{urine}$ values of MEOTs or BEOTs or in the AUCs of $nADC_{urine}$, for discriminating BEOTs from MEOTs (P = 0.10, 0.053 and 0.36, respectively). There was no significant difference between the AUCs of ADC_{tumor} and $nADC_{urine}$ with b factors of 800 s/mm² or 1000s/mm² (P = 0.19 and P = 0.69, respectively).

4. Discussion

In our study, patients with BEOTs were significantly younger than those with MEOTs, which is in agreement with previous reports [2]. DWI can provide information about the nuclear-to-cytoplasmic ratio, cellular density, and integrity of the cellular membrane based on the diffusion of water molecules [22]. This study showed that the solid components of BEOTs had significantly higher ADC_{tumor} values than those of MEOTs, which is consistent with the results of our previous study [13]. The increased cellularity and reduced extracellular space in malignant tumors restrict water molecule movement in tissue, thus leading to a low ADC value [12]. Additionally, we found that the ADC_{tumor} values of BEOTs and MEOTs were significantly higher in the same patients with b = 800 s/mm² (1.705×10^{-3} mm²/s, 0.913×10^{-3} mm²/s) than with b = 1000s/mm² (1.625×10^{-3} mm²/s, 0.874×10^{-3} mm²/s). Furthermore, the diagnostic performance of ADC_{tumor} in differentiating BEOTs from MEOTs was significantly better with a b factor of 1000s/mm² (AUC = 0.977) than with a b factor of 800 s/mm² (AUC = 0.892) in the same $Group_{b=}$800,1000 patients. Although no significant difference was found in the diagnostic performance of ADC_{tumor} between patients with a b factor of 800 s/mm² ($Group_{b=800}$, AUC = 0.960) and those with a b factor of 1000s/mm² ($Group_{b=1000}$, AUC = 0.966), the difference in age (50.0 years vs. 46.4 years, P = 0.02) may be one of the compromising factors, which led to different intragroup and intergroup results. Thus, we believe that the most reasonable explanation for the differences in ADC_{tumor} values and its differential AUCs was the different b factors. At lower b values, the ADC values are higher due to the dual effects of diffusion and perfusion. Higher b values reflect the relative true diffusion of tumors, while a lower signal-to-noise ratio may obstruct the detection of lesions. Then, the nADC can be applied to reduce the differences caused by different b values.

Several studies have indicated the superiority of nADC over ADC in diagnosing, grading or predicting endometrial carcinoma, prostate cancer, vesical urothelial carcinoma, metastatic lymph nodes and so on [19,22–25]. The spleen, liver, renal cortex, lumbar spine, paraspinal muscles, obturator internus, GMM and urine have been used as references [19,22–25]. In our study, the GMM, IM and urine were chosen as references because they were easy to observe and define in the pelvic cavity. The nADC may reduce interpatient variations and improve the reproducibility of the study [25]. The urine had the best intra- and interobserver agreements of the three references, which indicates that the $nADC_{urine}$ had the best reproducibility. The ADC_{urine} can be easily measured as urine displays a relatively homogeneous SI on ADC maps. Muscles are the most widely distributed tissues in the body, and they have been widely applied in clinical settings as normalization references. In our study, elliptical ROIs drawn as large as possible were placed on the areas of the muscles with homogeneous SI on the T2-weighted images, while trying to avoid fat, calcifications, and vascular structures. The relatively poor intra- and interobserver agreements and diagnostic performance of the ADC_{muscle} values may be due to the tiny vessels, muscular atrophy and increasing amount of adipose tissues in the muscular space that accompanies increasing age. Measurements of the ADC_{muscle} are prone to errors with different ROI areas and locations.

In our study, the ADC_{tumor}, $nADC_{GMM}$, $nADC_{IM}$ and $nADC_{urine}$ of BEOTs were all significantly higher than those of MEOTs at b = 800 s/mm² and 1000s/mm². Thus, the four ADC values were all able to differentiate BEOTs from MEOTs. Among the three references, $nADC_{urine}$ yielded the best diagnostic performance both at b = 800 s/mm² and at b = 1000s/mm². Wang et al. reported similar results that the AUC of $nADC_{urine}$ (0.995 ± 0.038) was significantly (P < 0.001) larger than that of $nADC_{GMM}$ (0.945 ± 0.039) and $nADC_{IM}$ (0.960 ± 0.034) in vesical urothelial carcinoma [25]. Muscles of patients with malignant tumors are usually edematous, with a high number of water molecules in the muscular space. Thus, the ADC values of muscle increase while $nADC_{GMM}$ and $nADC_{IM}$ decrease, which reduces the differences between BEOTs and MEOTs and in turn, reduces the diagnostic performances of the $nADC_{GMM}$ and $nADC_{IM}$ values. In addition, no significant difference was observed between the $nADC_{urine}$ with b values of 800 s/mm² and that with b values 1000s/mm². This result indicated that unlike ADC_{tumor}, the $nADC_{urine}$ was independent of the b values. Although there were no significant differences in diagnostic performance between ADC_{tumor} and $nADC_{urine}$ at b values of 800 s/mm² or 1000s/mm²,

Table 3
Comparisons of the ADC_{tumor} and nADC values (mean ± SD) in BEOTs and MEOTs.

ADC	b = 800 s/mm²			b = 1000s/mm²		
	BEOT (29)	MEOT (103)	P^* value	BEOT (36)	MEOT (96)	P^* value
ADC_{tumor}	1.599 ± 0.302	0.946 ± 0.202	< 0.001	1.564 ± 0.363	0.877 ± 0.161	< 0.001
$nADC_{GGM}$	1.698 ± 0.538	1.148 ± 0.858	0.001	1.771 ± 0.724	1.185 ± 0.432	< 0.001
$nADC_{IM}$	2.001 ± 1.042	1.546 ± 0.726	0.008	2.947 ± 2.235	1.750 ± 0.803	0.003
$nADC_{urine}$	0.585 ± 0.097	0.321 ± 0.064	< 0.001	0.579 ± 0.096	0.311 ± 0.067	< 0.001

ADC: apparent diffusion coefficient; nADC: normalized apparent diffusion coefficient; GMM: gluteus maximus muscle; IM: iliopsoas muscle; P^*: two independent-sample *t*-tests.

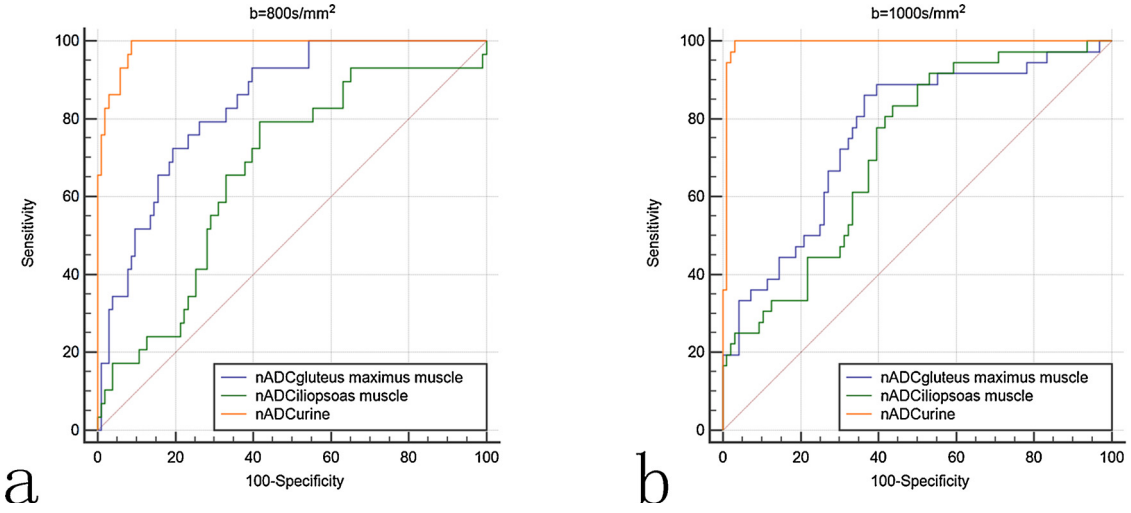

Fig. 3. ROC curves of the $nADC_{GMM}$, $nADC_{IM}$ and $nADC_{urine}$ with *b* values of 800 s/mm² (a) and 1000s/mm² (b) for distinguishing BEOTs from MEOTs. The AUCs of $nADC_{urine}$ at b = 800 and 1000s/mm² are significantly larger than those of $nADC_{GMM}$ ($P < 0.001$) and $nADC_{IM}$ ($P < 0.001$).

Table 4
Diagnostic performance of ADC_{tumor} and nADC at different *b* factors (n = 132).

	Sensitivity		Specificity		Threshold		AUC (95%CI)		
	b = 800	b = 1000	b = 800	b = 1000	b = 800	b = 1000	b = 800	b = 1000	$P^{\$}$ value
ADC_{tumor}	100%	83.33%	79.61%	96.87%	1.070	1.178	0.960 (0.911, 0.986)	0.966 (0.920, 0.990)	0.61
$nADC_{GMM}$	93.10%	86.11%	60.19%	63.54%	1.072	1.227	0.839 (0.765, 0.897)	0.763 (0.682, 0.833)	0.20
$nADC_{IM}$	79.31%	83.33%	58.25%	56.25%	1.368	1.511	0.666 (0.579, 0.746)	0.718 (0.634, 0.793)	0.48
$nADC_{urine}$	100%	100%	91.26%	96.87%	0.415	0.406	0.987 (0.950, 0.999)	0.992 (0.959, 1.000)	0.83
$P^{\$}$ value vs $nADC_{GM}$	–	–	–	–	–	–	< 0.001	< 0.001	–
vs $nADC_{IM}$	–	–	–	–	–	–	< 0.001	< 0.001	–
vs $nADC_{tumor}$	–	–	–	–	–	–	0.055	0.09	–

AUC: the area under the curve; CI: confidence interval; ADC_{tumor}: $\times 10^{-3}$ mm²/s; *b*: s/mm²; $P^{\$}$: Z test.

Table 5
The ADC_{tumor} and $nADC_{urine}$ values and their diagnostic performances with different diffusion gradient *b* factors in $Group_{b=}$800,1000 (n = 63).

Performance	b = 800 s/mm²	b = 1000s/mm²	*P* value
ADC_{tumor}			
BEOT	1.705 ± 0.322	1.625 ± 0.311	0.02*
MEOT	0.913 ± 0.191	0.874 ± 0.183	< 0.001*
Threshold	1.214	1.178	–
Sensitivity	75.00%	91.67%	–
Specificity	92.16%	96.08%	–
AUC (95% CI)	0.892 (0.788, 0.956)	0.977 (0.904, 0.998)	0.03$
$nADC_{urine}$			
BEOT	0.598 ± 0.131	0.624 ± 0.112	0.10*
MEOT	0.326 ± 0.075	0.322 ± 0.086	0.053*
Threshold	0.424	0.428	–
Sensitivity	91.67%	100%	–
Specificity	90.20%	90.20%	–
AUC (95% CI)	0.961 (0.879, 0.994)	0.985 (0.917, 1.000)	0.36$
P value vs ADC_{tumor}	0.19$	0.69$	

ADC_{tumor}: $\times 10^{-3}$ mm²/s; *: Wilcoxon signed-ranks test, $: Z test.

$nADC_{urine}$ was superior to ADC_{tumor} with better independence and stability.

Our study had several limitations. First, some histological subtypes of EOT were rare, and most of the included patients had serous tumors; this might influence the cut-off values for differential diagnosis. Therefore, selection bias was unavoidable. Second, our study was a single-institution and single-equipment research study. Further studies are needed to validate the feasibility of measuring $nADC_{urine}$ with different field-strength equipments, vendors and in different centers.

5. Conclusions

In summary, the ADC_{tumor}, $nADC_{GMM}$, $nADC_{IM}$ and $nADC_{urine}$ were all capable of differentiating BEOTs from MEOTs. The ADC_{tumor} was lower but its diagnostic performance was better at b = 1000s/mm² than at b = 800 s/mm². The $nADC_{urine}$ was the best of all nADC values and was superior to the ADC_{tumor} because of its stable performance in differentiating between BEOTs and MEOTs, regardless of if the *b* value was 800 s/mm² or 1000s/mm².

Funding

This work was supported by the National Natural Science Foundation of China [No. 81471628]; Science and Technology Commission Shanghai Municipality [No. 19411972000]; A New Round of Shanghai Medical Key Specialty Construction Project (Class A)-Medical Imaging [No. ZK2015A05].

References

[1] W.R. Hart, Borderline epithelial tumors of the ovary, Mod. Pathol. 182 (2005) S33–S50.
[2] D.M. Gershenson, Management of borderline ovarian tumours, Best Pract. Res. Clin. Obstet. Gynaecol. 41 (2017) 49–59.
[3] J.J. Lu, S. Pi, F.H. Ma, et al., Apparent diffusion coefficients measured using different regions of interest in differentiating borderline from malignant ovarian tumors, Acta Radiol. (2018) 17730840.
[4] M. Morotti, M.V. Menada, D.J. Gillott, et al., The preoperative diagnosis of borderline ovarian tumors: a review of current literature, Arch. Gynecol. Obstet. 285 (2012) 1103–1112.
[5] L. Barroilhet, A. Vitonis, T. Shipp, et al., Sonographic predictors of ovarian malignancy, J. Clin. Ultrasound 41 (2013) 269–274.
[6] T. Song, C.H. Choi, H. Kim, et al., Accuracy of frozen section diagnosis of borderline

ovarian tumors, Gynecol. Oncol. 122 (2011) 127–131.
[7] N.M. DeSouza, R. O'Neill, G.A. McIndoe, R. Dina, W.P. Soutter, et al., Borderline tumors of the ovary: CT and MRI features and tumor markers in differentiation from stage I disease, AJR Am. J. Roentgenol. 184 (2005) 999–1003.
[8] C.L. Bent, A. Sahdev, A.G. Rockall, et al., MRI appearances of borderline ovarian tumours, Clin. Radiol. 64 (2009) 430–438.
[9] S.H. Zhao, J.W. Qiang, G.F. Zhang, et al., MRI appearances of ovarian serous borderline tumor: pathological correlation, J. Magn. Reson. Imaging 40 (2014) 151–156.
[10] F.H. Ma, S.H. Zhao, J.W. Qiang, et al., MRI appearances of mucinous borderline ovarian tumors: pathological correlation, J. Magn. Reson. Imaging 40 (2014) 745–751.
[11] S.H. Zhao, J.W. Qiang, G.F. Zhang, et al., MRI in differentiating ovarian borderline from benign mucinous cystadenoma: pathological correlation, J. Magn. Reson. Imaging 39 (2014) 162–166.
[12] S. Pi, R. Cao, J.W. Qiang, et al., Utility of DWI with quantitative ADC values in ovarian tumors: a meta-analysis of diagnostic test performance, Acta Radiol. 59 (2018) 1386–1394.
[13] S.H. Zhao, J.W. Qiang, G.F. Zhang, et al., Diffusion-weighted MR imaging for differentiating borderline from malignant epithelial tumours of the ovary: pathological correlation, Eur. Radiol. 24 (2014) 2292–2299.
[14] Y. Kurata, A. Kido, Y. Moribata, et al., Diagnostic performance of MR imaging findings and quantitative values in the differentiation of seromucinous borderline tumour from endometriosis-related malignant ovarian tumour, Eur. Radiol. 27 (2017) 1695–1703.
[15] R. Mimura, F. Kato, K.K. Tha, et al., Comparison between borderline ovarian tumors and carcinomas using semi-automated histogram analysis of diffusion-weighted imaging: focusing on solid components, J. Radiol. 34 (2016) 229–237.
[16] H.M. Li, S.H. Zhao, J.W. Qiang, et al., Diffusion kurtosis imaging for differentiating borderline from malignant epithelial ovarian tumors: a correlation with Ki-67 expression, J. Magn. Reson. Imaging 46 (2017) 1499–1506.
[17] F.A. Denewar, M. Takeuchi, M. Urano, et al., Multiparametric MRI for differentiation of borderline ovarian tumors from stage I malignant epithelial ovarian tumors using multivariate logistic regression analysis, Eur. J. Radiol. 91 (2017) 116–123.
[18] S.O. Park, J.K. Kim, K.A. Kim, et al., Relative apparent diffusion coefficient: determination of reference site and validation of benefit for detecting metastatic lymph nodes in uterine cervical cancer, J. Magn. Reson. Imaging 29 (2009) 383–390.
[19] M. Barral, D. Sebbag-Sfez, C. Hoeffel, et al., Characterization of focal pancreatic lesions using normalized apparent diffusion coefficient at 1.5-Tesla: preliminary experience, Diagn. Interv. Imaging 94 (2013) 619–627.
[20] R.K. Do, H. Chandarana, E. Felker, et al., Diagnosis of liver fibrosis and cirrhosis with diffusion-weighted imaging: value of normalized apparent diffusion coefficient using the spleen as reference organ, AJR Am. J. Roentgenol. 195 (2010) 671–676.
[21] J. Oh, R.G. Henry, A. Pirzkall, et al., Survival analysis in patients with glioblastoma multiforme: predictive value of choline-to-N-acetylaspartate index, apparent diffusion coefficient, and relative cerebral blood volume, J. Magn. Reson. Imaging 19 (2004) 546–554.
[22] Y. Shen, F. Lv, Z. Xiao, et al., Utility of the relative apparent diffusion coefficient for preoperative assessment of low risk endometrial carcinoma, Clin. Image 56 (2019) 28–32.
[23] R. Itatani, T. Namimoto, A. Yoshimura, et al., Clinical utility of the normalized apparent diffusion coefficient for preoperative evaluation of the aggressiveness of prostate cancer, J. Radiol. 32 (2014) 685–691.
[24] J.S. Song, H.S. Kwak, J.H. Byon, et al., Diffusion-weighted MR imaging of upper abdominal organs at different time points: apparent diffusion coefficient normalization using a reference organ, J. Magn. Reson. Imaging 45 (2017) 1494–1501.
[25] H.J. Wang, M.H. Pui, Y. Guo, et al., Value of normalized apparent diffusion coefficient for estimating histological grade of vesical urothelial carcinoma, Clin. Radiol. 69 (2014) 727–731.